

Article

Thermal Properties and Thermal Degradation of Cellulose Tri-Stearate (CTs)

Feng-Yuan Huang

School of Chemical Engineering and Materials, Eastern Liaoning University, Dandong, Liaoning 118003, China; E-Mail: huangfengyuan@hotmail.com; Tel.: +86-415-3789735; Fax: +86-415-3789982

Received: 13 February 2012; in revised form: 2 April 2012 / Accepted: 5 April 2012 /

Published: 16 April 2012

Abstract: Cellulose tri-stearate (CTs) was synthesized employing trifluoroacetic anhydride (TFAA), stearic acid (SA), with microcrystal cellulose (MCC) and characterized with FT-IR and $^1\text{H-NMR}$. The degree of substitution of CTs was determined by the traditional saponification method and $^1\text{H-NMR}$. The thermal properties of CTs were investigated by the thermogravimetric analysis (TGA) under Ar flow in dynamic heating conditions. Thermal stability, activation energy, as well as the degradation mechanism of the decomposition process were revealed. The results showed that the thermal stability of CTs is superior to that of raw materials-MCC, and that the degradation of CTs in argon is a first-order weight loss; the initial decomposition temperature and the temperature corresponding to maximum degradation rate (T_p) increase with an increase in heating rate. The activation energy values were calculated with the Ozawa method, Coats-Redfern method and Kinssinger method, respectively. Analyses of experimental results suggest that the degradation mechanism $0.10 < \alpha < 0.80$ is F2 type, A3 for $\alpha < 0.1$, and R3 for $\alpha > 0.80$. The degradation mechanism of CTs in the whole conversion range is a complex mechanism, and is the combination of A3, F2 and R3.

Keywords: cellulose tri-stearate (CTs); thermal properties; thermal degradation mechanism; TGA

1. Introduction

Short-chain cellulose esters, such as cellulose acetate, cellulose acetate propionate and cellulose acetate butyrate, have been applied in fields such as coatings, plastics, composites, and laminates [1]. However, these short-chain cellulose esters have a narrow temperature window between melting temperature and decomposition; their applications have been limited. The long-chain cellulose esters (LCCEs) were considered to cover the shortages of short-chain cellulose esters. LCCEs were identified as potential biodegradable plastics for the enzymatically labile ester bond and the natural abundance of both cellulose and fatty acids [2]. Several methods have been developed to prepare LCCEs. These methods involved heterogeneous acylation by using acyl chloride, acid chlorides under vacuum or aliphatic acids with trifluoroacetic acid [3], and homogeneous acylation in DMAc/LiCl [4–6] or in ionic liquids [7,8]. Studies have shown that the maximum degree of substitution (DS) of LCCEs synthesized in ionic liquid system was up to approximately 2.0. It was obvious that the preparation of fully-functional cellulose esters in ionic liquids was unsuitable. In contrast, LCCEs with various DS values can be synthesized in DMAc/LiCl solution. However, during this process, the amount of reagents, including DMAc, fatty acids, and co-agents (*p*-toluenesulfonyl chloride or trifluoroacetic anhydride) consumed more, and the recovery of DMAc and LiCl were difficult. Generally, it was a time-consuming process to obtain fully substituted cellulose esters with fatty acids in DMA/LiCl. However, acylation of cellulose with acyl chlorides in DMA/LiCl by microwave irradiation gave esters with a DS approaching 3 in times as short as 3 min [9,10]. Microwave-induced acylation of cellulose by fatty acids or acyl chlorides was a rapid method to prepare LCCEs [9–11]. One of the potential disadvantages of the acylation of cellulose with acyl chlorides was the degradation of cellulose or cellulose esters for the existence of HCl produced in the reaction [3]. On the other hand, the synthesis of cellulose esters with trifluoroacetic anhydride (TFAA) [12] has many advantages, short reaction time, reagents saving, mild reaction conditions as well as easy separation of products. Hence, CTs was prepared in a heterogeneous system using TFAA as a promoter.

LCCEs had been considered as biodegradable plastics, and had the potential to become alternatives to the existing synthetic polymers. It was well known that a lot of plastics or polymers require heat processing to convert into final uses or undergo thermal effects, so their thermal properties have attracted much attention [13,14]. The thermal properties of cellulose esters were important from both practical and academic points of view. The glass transition temperatures and the melting points of cellulose esters have been investigated extensively [15–17]. The thermal stability of cellulose and short-chain cellulose esters have been studied [18]. The thermal degradation kinetic of non-fatty cellulose esters and partially esterified cellulose with long chain fatty acids were discussed by Jandura *et al.* [17] and Sairam *et al.* [19]. However, thermal stability and thermal degradation kinetics of cellulose tri-stearate (CTs) have not been reported. The objective of this work was to study the thermal stability and thermal decomposition kinetics of CTs by using a dynamic TG analysis, and reveal the mechanism of thermal degradation of CTs.

2. Experimental Section

2.1. Materials

The cellulose used was Microcrystal Cellulose (MCC) powder (OurChem, DP = 235). Special grade trifluoroacetic anhydride (TFAA) and stearic acid (SA) were used for the acylation of cellulose. Reagent grade ethanol and other reagents were used without being further purified.

2.2. Synthesis of CTs

CTs was synthesized following Morooka's method [15] with some modifications. TFAA and stearic acid (mole ratio of fatty acid to TFAA was 1.1) were mixed together in a 250 mL three-neck flask equipped with a condenser and stirred mildly at 50 °C for 20 min to form the mixed acid anhydride. Pre-dried MCC powder was added to this solution and stirred mildly at 50 °C for a certain time. During the reaction, chloroform was added as dissolvent. The reaction mixtures were poured into an excess amount of ethanol, and the precipitates were filtered and washed with methanol (50 mL per gram of MCC) three times. Then, Soxhlet extraction with ethanol was carried out for 24 h. Finally, the polymers were dried at 50 °C for 24 h under vacuum to yield products.

2.3. Characterizations of CTs

2.3.1. FTIR

FT-IR spectra were measured on a PerkinElmer Spectrum 100 using the KBr pellet technique for all samples. KBr tablets were dried at 105 °C for 1h to remove moisture prior to the measurement.

2.3.2. ¹H-NMR

¹H-NMR spectrum was acquired on a Bruker Advance 400 MHz spectrometer with 16 scans for by using a standard 5-mm probe at room temperature in CDCl₃ to determine the DS.

2.3.3. Degree of Substitution (DS)

DS was determined by the traditional saponification method. A purified sample (0.5 g) was stirred for 30 min in 40 mL of aqueous ethanol (70%). After the addition of 40 mL of a 0.25 M NaOH aqueous solution, the stirring was continued for 48 h at 50 °C. The un-reacted NaOH was back titrated with 0.25 M aqueous HCl.

2.3.4. Thermal Analysis

Thermogravimetric analysis was conducted on a NETZSCH STA 449C TG/DSC. As mentioned in 2.2, MCC was also pre-dried in 105 °C under vacuum before measurement. A first scanning was run from 30 to 105 °C to erase any thermal events that might have occurred during the preparation and storage of the samples. After rapid cooling to 30 °C, the temperature was scanned between 30 °C and

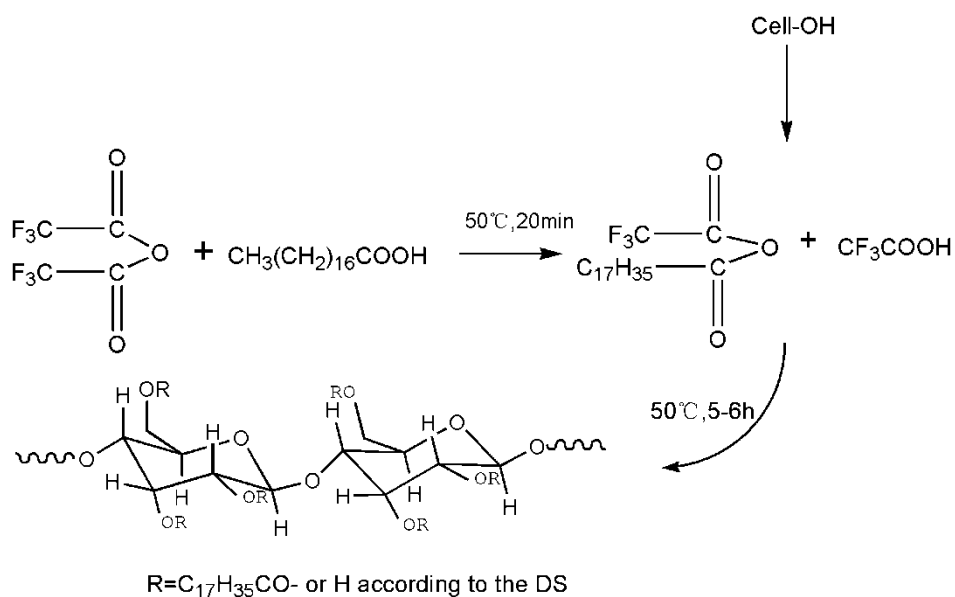
450 °C at heating rates of 10, 15, 20, and 25 K/min, respectively. All samples were in a 25 mL/min flow of Ar.

3. Results and Discussion

3.1. Synthesis and Characterization of CTs

The esterification process for CTs preparation involves two steps according to the process used for cellulose acylates [15]. The first stage involves the formation of mixed acid anhydride. The reaction takes place easily at 50 °C. *ca.* 20 min was enough to complete the first stage. The mixture becomes a pale-yellow color. In the second stage, esterification stage, pre-dried MCC was added into the former solution, and a heterogeneous system was obtained. However, with the development of reaction, a phase transfer can be seen, a homogeneous system gradually formed. The color did not significantly change. Table 1 shows the conditions of synthesis of CTs and the DS of products. The reactions that take place during these stages and the procedure used for the synthesis of CTs are presented in Figure 1. The difference in DS value between sample 1 and sample 3 is 0.15; the increase of DS is due to the addition of chloroform. Research results show that when the degree of substitution of LCCEs is greater than 1.4, the ester can dissolve in chloroform. Thus, the addition of chloroform can dissolve the reactants (except cellulose) and product, make the viscosity reduced and benefit for the contacting of cellulose and mixed acid anhydride. Toluene also has the same effect. The addition of solvents can save reagents effectively, and make a nearly quantitative reaction between cellulose and mixed acid anhydride reality. The reagents consumed were less than those in reference [15].

Figure 1. Synthetic route to cellulose stearate.



A comparative FT-IR analysis of MCC (a), cellulose state (DS = 2.45, b) and CTs (c) clearly shows the relative efficiency of acylation (Figure 2). For cellulose stearate (Figure 2b) and CTs (Figure 2c), a decrease in the intensity and a shift of the characteristic band for hydroxyl groups at 3448 cm⁻¹ were observed relative to the spectra of the MCC (Figure 1a), indicating that a number of OH groups were substituted. In addition to this phenomenon, we also observed an increase in the intensities of the

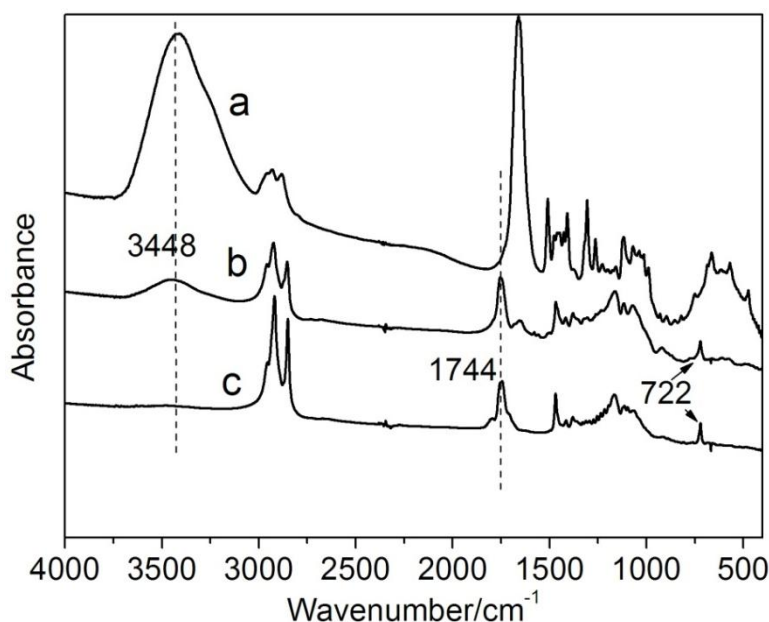
characteristic bands of CH alkyl bonds at 2800–2900 cm^{-1} (CH anti-symmetric and symmetric stretching of CH_2 and CH_3). There were two new bands in the spectrum: the first band appeared at 1744 cm^{-1} (C=O stretching), corresponding to the vibration of carbonyl ester groups, and the second band appeared at 722 cm^{-1} (CH_2 rocking) which is characteristic of at least four linearly connected CH_2 groups.

Table 1. Reaction conditions and degree of substitution (DS) of cellulose stearate.

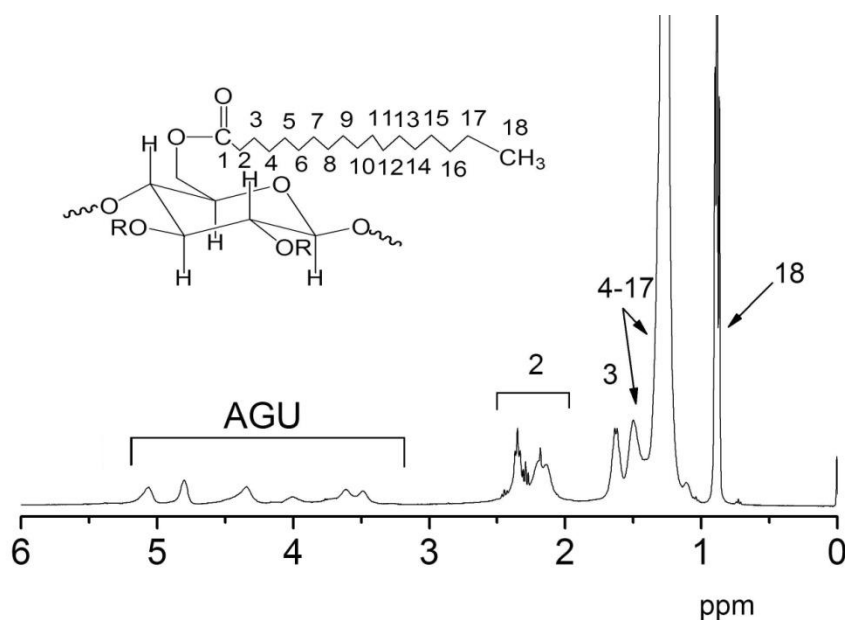
No.	Molar ratio of AGU: TFAA: SA ^a	Reaction temperature °C	Reaction time h	Solvent added	WI ^c %	Yield %	DS
1	1:3.3:3.63	50	5	/	256	89	2.80
2	1:3.3:3.63	50	4	Chloroform/50 mL	261	88	2.85
3	1:3.3:3.63	50	5	Chloroform/50 mL	313	97	2.95 2.99 ^d
4	1:3.3:3.63	50	5	Toluene/50 mL	276	90	2.90
5 ^b	1:10:11	50	5	/	308	92	2.97
6	1:2.6:2.9	50	5	Chloroform/100 mL	209	95	2.45

^a 2 g cellulose, 167 mmol AGU; ^b see reference [15]; ^c weight increase; ^d determined with ¹H-NMR.

Figure 2. FTIR of microcrystal cellulose (MCC) (a), cellulose stearate (DS = 2.45) (b) and Cellulose tri-stearate (CTs) (c).



CTs has a good solubility in CDCl_3 , and the ¹H-NMR spectrum in CDCl_3 is shown in Figure 3. The well-resolved spectrum shows a separate signal for all the AGU protons in the region $\delta = 3.46\text{--}5.08$ ppm. The protons on the aliphatic chain appear at 0.88 ppm (t, 3H, C18), 1.25–1.54 ppm (m, broad peaks, 28H, C4–C17), 1.61 ppm (m, 2H, C3), and 2.16–2.35 ppm (m, broad peaks, 2H, C2), respectively. The DS of 2.99, calculated from the ¹H-NMR spectrum of the CTs, confirms the fully-esterification of cellulose.

Figure 3. $^1\text{H-NMR}$ of CTs.

3.2. Thermal Properties of CTs

Figure 4 shows dynamic TG curves of MCC and CTs at heating rate of 10 K/min in Ar. The thermal degradation of MCC consists of a series of degradation reaction, such as dehydration at *ca.* 100 °C, this weight loss was mainly due to the evaporation of bonding water on MCC and the thermal pyrolysis of the cellulose skeleton at ~300 °C. However, there was very little hydroxyl on CTs' molecular chain, which means that CTs was hydrophobic. Therefore, there has not significant weight-loss at *ca.*100 °C. The temperature of α equal to 5% for CTs was 320 °C, while that for MCC was only 296 °C. The temperature corresponding to maximum degradation rates (T_p) for CTs was 371 °C, while that for MCC was 344.6 °C. Therefore, thermal stability of CTs is superior to that of MCC. Obviously, the presence of the substituted groups on the cellulose skeleton is expected to influence the thermo-stability. The results can be explained from the difference between the structure of MCC and CTs. The long fatty ester groups on the cellulose skeleton can be in a regular arrangement and form a new ordered structure; even the side chain can form a new crystal structure, so as to improve the thermal stability of CTs. Side-chain crystallization of long *n*-alkyl side chains on poly(*n*-alkyl thiophenes), which has stiff backbones, had been found by Hsu *et al.* [20]. Sealey *et al.* demonstrated favorable conformation for side-chain crystallization of cellulose eicosanoate (C20) with computer simulation [16]. The char residue of CTs is less than that of MCC. Compared with MCC, stearic acid ester occupies the major proportion in the same quality of CTs, while the ester groups degraded and easily produced volatiles; therefore the char residue of CTs is lower than that of MCC. In summary, the thermal stability of CTs was significantly superior to that of MCC.

Figure 5 shows TG (Figure 5a) and DTG (Figure 5b) curves of CTs corresponding to dynamic experiments carried out at 10, 15, 20, and 25 K/min with argon flow rate 25 mL/min. It is clear from the DTG plots that the T_p values shift upwards with increasing heating rate. An increase of 19 °C in the initial thermal decomposition temperature is measured. Obviously, there is a strong influence of heating rate for the degradation of CTs.

Figure 4. Thermogravimetric (TG) curves of CTs and MCC at 10 K/min.

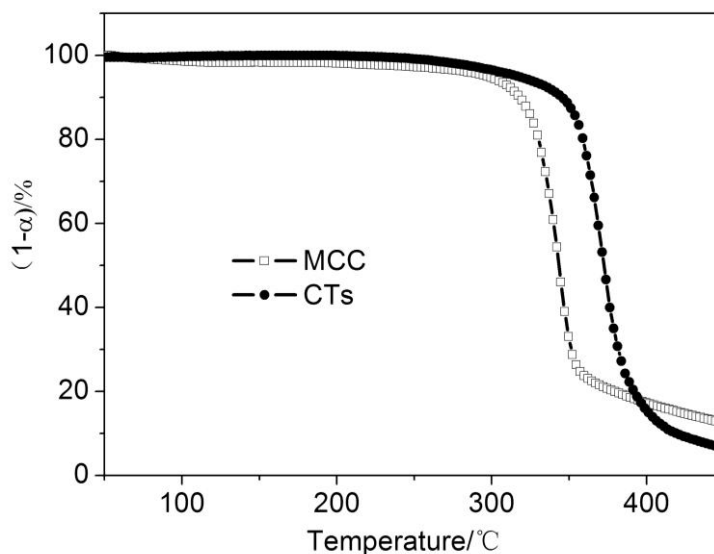
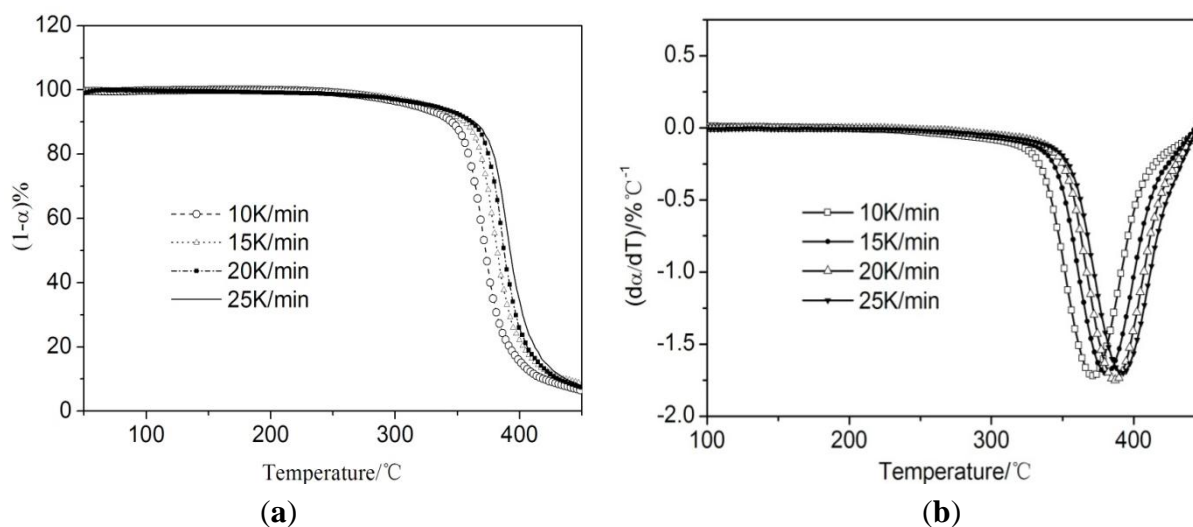


Figure 5. TG/DTG curves of (a) CTs and (b) MCC.



3.3. Thermogravimetric Analysis of CTs

In order to analyze more deeply the degradation mechanism of CTs, it is important that activation energy E and conversion function $g(\alpha)$ are evaluated. The relationship between kinetic parameters can be found by using the mass-loss curves recorded in TG dynamic thermograms. The thermogravimetric curves of CTs heated in Ar at different heating rates are shown in Figure 5.

Two methods, Ozawa [21] (also known as the FWO method) and Kissinger [22], have investigated the thermal degradation kinetic parameters of CTs. The Coats-Redfern method [23] was used to determine the mechanism of the degradation of CTs after the activation energy obtained.

The Ozawa method is an integral method, using multiple heating rates curves to calculate kinetic parameters, and does not involve reaction mechanism hypotheses. According to the Ozawa method, Equation (1) can be obtained. In Equation (1), the $\ln[F(\alpha)]$ is constant for the same α , and the plot of

$\ln\beta$ vs. $1000/T$ should be a straight line, thus, the activation energy can be calculated from the slope, which is $-1.0516 E/R$.

$$\ln \beta = \ln\left(\frac{AE}{R}\right) - 5.3305 - 1.0516 \frac{E}{RT} - \ln[F(\alpha)] \tag{1}$$

where β is the heating rate, T is the temperature, A is the pre-exponential factor, α is the conversion, and E is the activation energy.

Some of the Ozawa plots are shown in Figure 6, and all data are summarized in Table 2. Figure 6 shows the data fitted to straight lines, with a correlation coefficient greater than 0.990. These lines are nearly parallel in the conversion range of $0.10 < \alpha < 0.80$, thus indicating the applicability of Ozawa method to the present system. As seen from Table 2, when the conversion was less than 10%, the activation energy gradually increased, indicating that weight loss becomes increasingly difficult. However, for conversion in the 10–80% range, values of activation energy can be considered essentially the same, and the average activation energy value was 152.8 ± 8.98 KJ/mol. E does not significantly change for conversions between 0.10 and 0.80, indicating that the degradation of CTs takes place through the cleavage of linkages with similar bond energies.

Figure 6. The plots of $\ln(\beta)$ vs. $1000/T$. (a) $\alpha < 0.7$ and $\alpha > 0.8$; (b) $0.10 < \alpha < 0.80$.

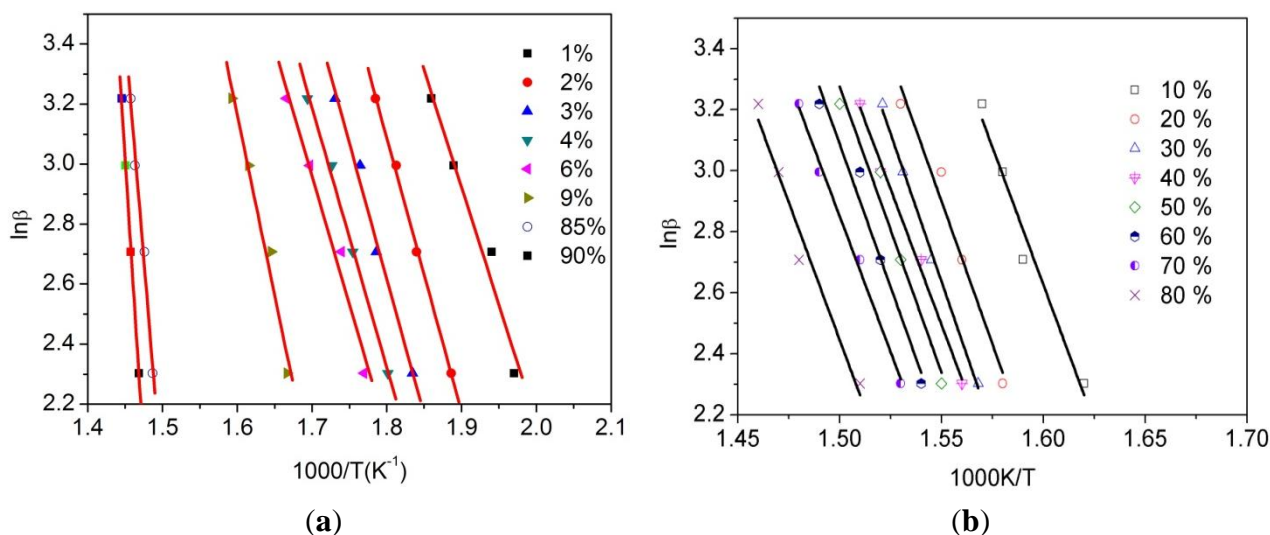
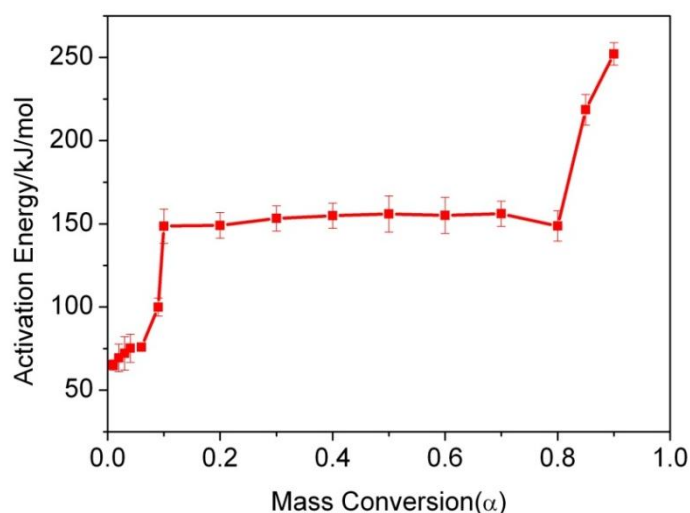


Table 2. Activation energies obtained using the Ozawa method.

$\alpha/\%$	1	2	3	4	6	9
Ea(KJ/mol)	65.0 ± 3.1	69.4 ± 8.3	72.1 ± 10.1	75.2 ± 8.5	75.9 ± 2.2	99.9 ± 5.4
R	0.9942	0.9603	0.9587	0.9487	0.9972	0.9843
$\alpha/\%$	10	20	30	40	50	60
Ea(KJ/mol)	148.6 ± 10.25	149.1 ± 7.79	153.3 ± 7.58	154.9 ± 7.58	156.0 ± 10.93	155.1 ± 10.93
R	0.9906	0.9957	0.9965	0.9965	0.9933	0.9923
$\alpha/\%$	70	80	85	90		
Ea(KJ/mol)	156.1 ± 7.58	148.7 ± 9.16	218.6 ± 9.25	252.1 ± 6.72		
R	0.9965	0.9947	0.9926	0.9966		

Figure 7. Dependence of the activation energy on mass conversion, as calculated with the Ozawa method.



From Table 2 and Figure 7, we can see that the dependence of the active energy on α can be separated into three distinct regions for the thermal degradation of CTs. The first region is for values of $\alpha \leq 0.1$, a small increase in the active energy. The second region is between $0.1 < \alpha < 0.8$, where the activation energy can be considered as a constant value. The third region is for $\alpha > 0.8$, where a rapid increase of the activation energy is observed. The change of activation energy with α indicates that a complex reaction mechanism exists for the thermal degradation of CTs. According to Figure 7, there may be three different mechanisms during the decomposition of CTs. The first mechanism corresponds to the part where small loss appears; the second part, where the substantial mass loss takes place, is owed to the chief decomposition mechanism; the third mechanism corresponds to the final part of degradation; each mechanism presenting different activation energies. This is in good agreement with the results of many aliphatic polyesters [24–27].

In order to investigate the degradation mechanism of CTs in detail, the Coats and Redfern method was used to calculate the activation energy. The activation energy for every $g(\alpha)$ function listed in Table 3 can be obtained at constant heating rates from fitting of $\ln[g(\alpha)/T^2]$ vs. $1000/T$ plots. The Coats–Redfern method can be written as Equation (2):

$$\ln \frac{g(\alpha)}{T^2} = \ln \frac{AR}{\beta E} - \frac{E}{RT} \quad (2)$$

Comparing the activation energy values in Table 2 and in Table 3, we can see that, at the early degradation stage, namely $\alpha < 0.1$, the degradation mechanism may match the A2 or A3, and tend towards A3 because the value obtained from A3 is very close to those from the Ozawa method. In the main degradation process, or $0.1 < \alpha < 0.8$, the mechanism may match the F2 mechanism well; in the final stage, $\alpha > 0.8$, the degradation mechanism may match R3.

Table 3. Algebraic expressions for $g(\alpha)$ for the most used mechanisms and activation energies obtained using the Coats–Redfern method.

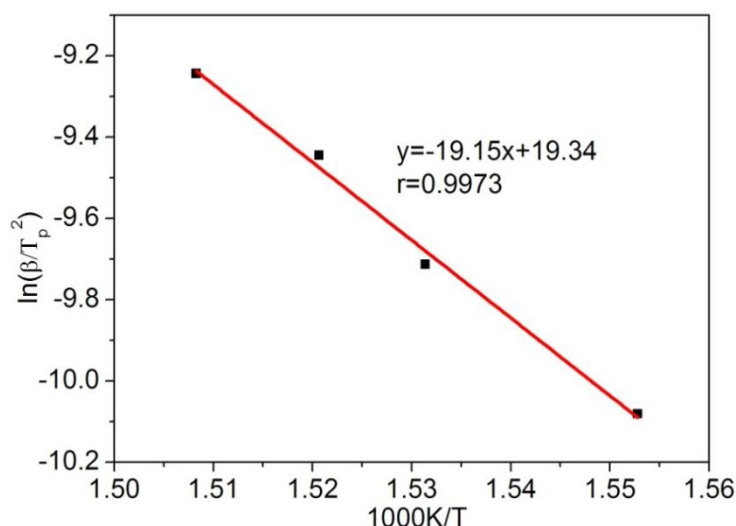
Mechanism	$\beta(\text{K/min})$	10		15		20		25	
		E	R ²						
A2	$-\ln(1 - \alpha)^{1/2}$	106	0.9903	116	0.9891	121	0.9916	127	0.981
A3	$-\ln(1 - \alpha)^{1/3}$	67	0.9892	73	0.9881	77	0.9907	81	0.979
A4	$-\ln(1 - \alpha)^{1/4}$	48	0.9879	52	0.9869	55	0.9898	58	0.9768
R1	α	155	0.9875	168	0.9898	185	0.9936	207	0.9892
R2	$1 - (1 - \alpha)^{1/2}$	186	0.9744	193	0.9705	202	0.9848	217	0.9727
R3	$1 - (1 - \alpha)^{1/3}$	205	0.9979	220	0.9935	236	0.9971	243	0.9887
D1	α^2	347	0.9922	359	0.9872	382	0.9875	407	0.9917
D2	$(1 - \alpha)\ln(1 - \alpha) + \alpha$	320	0.9966	396	0.9978	422	0.9919	441	0.9976
D3	$[1 - (1 - \alpha)^{1/3}]^2$	390	0.9974	407	0.9992	440	0.9983	467	0.9897
D4	$(1 - 2/3\alpha) - (1 - \alpha)^{2/3}$	385	0.9878	421	0.9889	439	0.9856	473	0.9912
F1	$-\ln(1 - \alpha)$	223	0.9921	242	0.9987	253	0.9993	267	0.9987
F2	$1/(1 - \alpha)$	153	0.9974	156	0.9987	159	0.9992	160	0.9987
F3	$1/(1 - \alpha)^2$	290	0.9914	300	0.9763	322	0.9668	328	0.9940

For comparative purposes, the activation energy in the main degradation stage also was calculated by the Kissinger method. The T_p was applied to calculate the activation energy in this method, though the Kissinger method was suitable to explain the mechanism for the chief thermal degradation region. The Kissinger method has been used in the literature to determine the activation energy of solid-state reactions from plots of the $\ln(\beta/T_p^2)$ vs. $1000/T_p$ in constant heating rate experiments. The activation energy can be determined by the Kissinger method without precise knowledge of the reaction mechanism, using Equation (3):

$$\ln\left(\frac{\beta}{T_p^2}\right) = \ln\left(\frac{AR}{E}\right) - \frac{E}{RT_p} \quad (3)$$

where β , A , E , and T_p are the known meanings. Figure 8 shows that the activation energy obtained is 159.2 KJ/mol, and the correlation coefficient is 0.9973. The value is slightly higher than that calculated with the Ozawa method; however, it falls within the scope of former's deviation. Thus, the activation energy calculated from the Kissinger method was consistent with that from the Ozawa method.

For this study, we have used the same conversion values in the whole α range. Table 3 also shows activation energies and correlations for conversions at heating rate 10, 15, 20, and 25 K/min, respectively. At all heating rates, the activation energy values calculated with F2 type (Random nucleation with two nuclei on the individual particle) mechanism for the chief stage ($0.1 < \alpha < 0.8$) are in better agreement with those obtained using the former two methods. Also, from this table it can be seen that the optimum heating rate value is 20 K/min, at which the activation energy corresponding to F2 mechanism is 159 KJ/mol, very close to 159.2 KJ/mol obtained by Kissinger method. These facts strongly suggest that the solid state thermodegradation mechanism followed by CTs in $0.1 < \alpha < 0.8$ is an F2 type. Therefore, the thermal degradation mechanism for CTs may be the combination of A3, F2 and R3.

Figure 8. The plot of $\lg(\beta/T_p^2)$ vs. $1000/T$.

4. Conclusions

CTs was synthesized employing trifluoroacetic anhydride (TFAA), stearic acid (SA), with MCC in a heterogeneous system. FTIR, ¹H-NMR and DS determination were confirmed the structure of fully-functional cellulose ester. The study of TG curves indicated that the thermal stability of CTs was significantly superior to that of MCC. The improvement of thermal stability was due to the regular arrangement of the side chains. The activation energy for the main stage (conversion value in 10–80%) of the decomposition of CTs was calculated with the Ozawa method and the Kissinger method, respectively. The value from the Kissinger method, 159.2 KJ/mol, was consistent with that from the Ozawa method, 152.8 ± 8.98 KJ/mol. Combined with the Ozawa method, the Coats-Redfern method and the Kissinger method, the degradation mechanism of CTs is the combination of A3, F2 and R3.

Acknowledgments

This work was supported by the Doctoral Scientific Research Foundation of Liaoning Province of China (No.20101043).

References

1. Edgar, K.J.; Buchanan, C.M.; Debenham, J.S.; Rundquist, P.A.; Seiler, B.D.; Shelton, M.C.; Tindall, D. Advances in cellulose ester performance and application. *Prog. Polym. Sci.* **2001**, *26*, 1605–1688.
2. Kwatra, H.S.; Caruthers, J.M.; Tao, B.Y. Synthesis of long chain fatty acids esterified onto cellulose via the vacuum-acid chloride process. *Ind. Eng. Chem. Res.* **1992**, *31*, 2647–2651.
3. Heinze, T.; Liebert, T. Unconventional methods in cellulose functionalization. *Prog. Polym. Sci.* **2001**, *26*, 1689–1762.
4. Crépy, L.; Chaveriat, L.; Banoub, J.; Martin, P.; Joly, N. Synthesis of cellulose fatty esters as plastics-influence of the degree of substitution and the fatty chain length on mechanical properties. *ChemSusChem* **2009**, *2*, 165–170.

5. Huang, F.Y.; Yu, Y.; Wu, X.J. Characterization and Properties of Cellulose Oleate. *Adv. Mater. Res.* **2011**, *197–198*, 1306–1309.
6. Heinze, T.; Liebert, T.F.; Pfeiffer, K.S.; Hussain, M.A. Unconventional cellulose ester: Synthesis, characterization and structure-property relations. *Cellulose* **2003**, *10*, 283–296.
7. Granstrom, M.; Kavakka, J.; King, A.; Majoinen, J.; Makela, V.; Helaja, J.; Hietala, S.; Virtanen, T.; Maunu, S.L.; Argyropoulos, D.S.; Kilpelainen, I. Tosylation and acylation of cellulose in 1-allyl-3-methylimidazolium chloride. *Cellulose* **2008**, *15*, 481–488.
8. Barthel, S.; Heinze, T. Acylation and carbanilation of cellulose in ionic liquids. *Green Chem.* **2006**, *8*, 301–306.
9. Memmi, A.; Granet, R.; Gahbiche, M.A.; Fekih, A.; Bakhrouf, A.; Krausz, P. Fatty esters of cellulose from olive pomace and barley bran: improved mechanical properties by metathesis crosslinking. *J. Appl. Polym. Sci.* **2006**, *101*, 751–755.
10. Satgé, C.; Verneuil, B.; Branland, P.; Granet, R.; Krausz, P.; Rozier, J.; Petit, C. Rapid homogeneous esterification of cellulose induced by microwave irradiation. *Carbohydr. Polym.* **2002**, *49*, 373–376.
11. Joly, N.; Granet, R.; Branland, P.; Verneuil, B.; Krausz, P. New methods for acylation of pure and sawdust-extracted cellulose by fatty acid derivatives—Thermal and mechanical analyses of cellulose-based plastic films. *J. Appl. Polym. Sci.* **2005**, *97*, 1266–1278.
12. Arni, P.C.; Gray, J.D.; Scougall, R.K. Chemical modification of wood. I. Use of trifluoroacetic anhydride in the esterification of wood by carboxylic acids. *J. Appl. Chem.* **1961**, *11*, 157–163.
13. Roy, P.K.; Surekha, P.; Rajagopal, C.; Choudhary, V. Thermal degradation studies of LDPE containing cobalt stearate as pro-oxidant. *Express Polym. Lett.* **2007**, *4*, 208–216.
14. Wang, H.M.; Tao, X.M.; Newton, E. Thermal degradation kinetics and lifetime prediction of a luminescent conducting polymer. *Polym. Int.* **2004**, *53*, 20–26.
15. Morooka, T.; Norimoto, M.; Yamada, T. Dielectric properties of cellulose acylates. *J. Appl. Polym. Sci.* **1984**, *29*, 3981–3990.
16. Sealey, J.E.; Samaranayake, G.; Todd, J.G.; Glasser, W.G. Novel cellulose derivatives. IV. Preparation and thermal analysis of waxy esters of cellulose. *J. Polym. Sci. B Polym. Phys.* **1996**, *34*, 1613–1620.
17. Jandura, P.; Riedl, B.; Kokta, B.V. Thermal degradation behavior of cellulose fibers partially esterified with some long chain organic acids. *Polym. Degrad. Stabil.* **2000**, *70*, 387–394.
18. Huang, M.R.; Li, X.G. Thermal degradation of cellulose and cellulose esters. *J. Appl. Polym. Sci.* **1998**, *68*, 293–304.
19. Sairam, M.; Sreedhar, B.; Mohan Rao, D.V.; Srinivasan, P. Synthesis and thermal degradation kinetics of cellulose esters. *Polym. Adv. Technol.* **2003**, *14*, 477–485.
20. Hsu, W.P.; Levon, K.; Ho, K.S.; Myerson, A.S.; Kwei, T.K. Side chain order in poly(3-Alkyl Thiophanes). *Macromolecules* **1993**, *26*, 1318–1323.
21. Ozawa, T.A. New method of analyzing thermogravimetric data. *Bull. Chem. Soc. Jpn.* **1965**, *38*, 1881–1886.
22. Kissinger, H.E. Reaction kinetics in differential thermal analysis. *Anal. Chem.* **1957**, *29*, 1702–1706.

23. Coats, A.W.; Redfern, J.P. Kinetic parameters from thermogravimetric data. *Nature* **1964**, *201*, 68–69.
24. Chrissafis, K.; Paraskevopoulos, K.M.; Bikiaris, D.N. Thermal degradation kinetics of the biodegradable aliphatic polyester, poly(propylene succinate). *Polym. Degrad. Stabil.* **2006**, *91*, 60–68.
25. Chrissafis, K.; Paraskevopoulos, K.M.; Bikiaris, D.N. Effect of molecular weight on thermal degradation mechanism of the biodegradable polyester poly(ethylene succinate). *Thermochim. Acta* **2006**, *440*, 166–175.
26. Chrissafis, K.; Paraskevopoulos, K.M.; Bikiaris, D. Thermal degradation kinetics and decomposition mechanism of two new aliphatic biodegradable polyesters poly(propylene glutarate) and poly(propylene suberate). *Thermochim. Acta* **2010**, *505*, 59–68.
27. Chrissafis, K.; Paraskevopoulos, K.M.; Papageorgiou, G.Z.; Bikiaris, D.N. Thermal decomposition of poly(propylene sebacate) and poly(propylene azelate) biodegradable polyesters: Evaluation of mechanisms using TGA, FTIR and GC/MS. *J. Anal. Appl. Pyrol.* **2011**, *92*, 123–130.

© 2012 by the authors; licensee MDPI, Basel, Switzerland. This article is an open access article distributed under the terms and conditions of the Creative Commons Attribution license (<http://creativecommons.org/licenses/by/3.0/>).